

Superconductivity with the Meron-Cluster Algorithm

J.C. Osborn^a *

^aDepartment of Physics, Box 90305, Duke University, Durham, NC 27708, U.S.A.

The meron-cluster algorithm was previously used to extensively study the physics associated with the spontaneous breaking of a discrete symmetry. We recently discovered that a larger class of models with spontaneous breaking of continuous symmetries can also be simulated using the meron-cluster algorithm. Here we study one of these new models which belongs to the attractive Hubbard model family. In particular we study the spontaneous breaking of the $U(1)$ fermion number symmetry in two dimensions and find clear evidence for a Kosterlitz-Thouless transition to a superconducting phase.

1. Introduction

For over a decade there has been a lot of interest in performing numerical simulations of strongly correlated fermionic systems. A recently discovered method for solving the sign problem inherent in such simulations is the meron-cluster algorithm [1]. A new reference configuration allows us to explore a larger class of models with this method. The model we study here is a variant of the attractive Hubbard model.

The attractive Hubbard model has received a lot of attention as a toy model for superconductivity. It is a very simplistic model since the attraction between fermions is explicitly included, instead of arising from some more subtle mechanism. In that respect it is perhaps more closely related to the case of color superconductivity in QCD. It is still useful as a model for high- T_c superconductors since at intermediate attraction strength they both exhibit pairing at temperatures above the superconducting transition [2].

Despite the Hubbard model's simplicity, numerical attempts to verify the properties of a Kosterlitz-Thouless (KT) transition are inconsistent [3]. The main reason seems to be the fairly small lattice size restriction imposed by conventional fermionic Monte Carlo methods. Since the meron-cluster algorithm scales very efficiently with lattice volume, we are able to go to large system sizes needed to accurately test finite size

scaling formulas. Another advantage comes from performing the simulation directly in the fermion occupation basis, thus allowing very simple access to a wide range of observables.

2. The Model

We study a model of fermions with spin on a lattice in two spatial dimensions. The Hamilton operator can be written as

$$H = \sum_{\langle x,y \rangle} h_{xy} + \sum_x h_x, \quad (1)$$

with a nearest neighbor interaction

$$\begin{aligned} h_{xy} &= \sum_s (c_{x,s}^\dagger c_{y,s} + c_{y,s}^\dagger c_{x,s}) \\ &\times [(n_{xy} - 1)(n_{xy} - 3) + \Delta(n_{xy} - 2)] \\ &+ 2(1 + \Delta) [\vec{S}_x \cdot \vec{S}_y + \vec{J}_x \cdot \vec{J}_y] - 4\Delta J_x^3 J_y^3 \\ &- 4 \left[(n_{x,\uparrow} - \frac{1}{2})(n_{x,\downarrow} - \frac{1}{2}) + \frac{\Delta}{4} \right] \\ &\times \left[(n_{y,\uparrow} - \frac{1}{2})(n_{y,\downarrow} - \frac{1}{2}) + \frac{\Delta}{4} \right], \quad (2) \end{aligned}$$

and an on-site term

$$h_x = -U (n_{x,\uparrow} - \frac{1}{2})(n_{x,\downarrow} - \frac{1}{2}) - \mu n_x. \quad (3)$$

We also define the number operators

$$\begin{aligned} n_{x,s} &= c_{x,s}^\dagger c_{x,s} \quad (s = \uparrow, \downarrow), \\ n_x &= n_{x,\uparrow} + n_{x,\downarrow}, \quad n_{xy} = n_x + n_y, \quad (4) \end{aligned}$$

*This work was done in collaboration with S. Chandrasekharan under DOE grant DE-FG02-96ER40945.

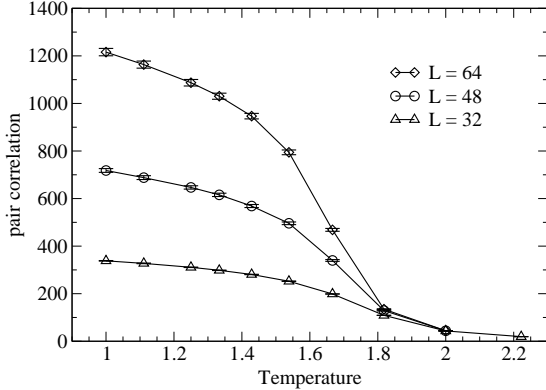


Figure 1. Pair correlation versus temperature for $U = 8$ and $\Delta = 1$.

along with the on-site spin

$$\vec{S}_x = \frac{1}{2} c_{x,s}^\dagger \vec{\sigma}_{s,s'} c_{x,s'} \quad (5)$$

and pseudo-spin operators

$$\begin{aligned} J_x^+ &= (-1)^x c_{x,\uparrow}^\dagger c_{x,\downarrow}^\dagger, \quad J_x^- = (J_x^+)^\dagger, \\ J_x^3 &= \frac{1}{2} [n_x^\uparrow + n_x^\downarrow - 1]. \end{aligned} \quad (6)$$

The term containing U serves to bind the fermions with opposite spin together on a lattice site. In the limit as $U \rightarrow \infty$ the model becomes bosonic and can be mapped onto the anisotropic quantum Heisenberg model. As U decreases the model becomes increasingly fermionic, as in the attractive Hubbard model. However, at $U = 0$ we still have a strongly interacting system due to the additional terms present.

In spite of these additional factors, we still expect this model to behave similarly to the attractive Hubbard model since they both possess the same symmetries. The important symmetries are the $SU(2)_s$ spin group generated by the standard fermionic spin operator $\vec{S} = \sum_x \vec{S}_x$, and the $SU(2)_c$ charge symmetry generated by the pseudo-spin operator $\vec{J} = \sum_x \vec{J}_x$. The $SU(2)_s$ group is always a symmetry of the Hamiltonian, but the $SU(2)_c$ group is broken down to the $U(1)_c$ particle number group if either μ or Δ are nonzero. The remaining $U(1)_c$ symmetry can then undergo a Kosterlitz-Thouless transition in two dimensions.

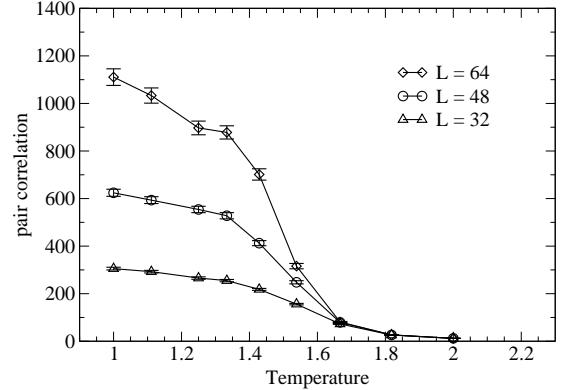


Figure 2. Pair correlation versus temperature for $U = 0$ and $\Delta = 1$.

Here we will only consider the case where the $SU(2)_c$ is broken by $\Delta \neq 0$ at half filling ($\mu = 0$) as a test of the model and our simulations. We will study the more physically relevant case of $\mu \neq 0$ elsewhere [4].

3. Simulation Method

The meron-cluster algorithm uses clusters in the standard path integral formulation of a quantum model to solve the sign problem arising from fermion permutations. It has been presented in detail for a variety of models [1,5,6]. Here we will only outline the extension to this model.

We chose this particular model because of its simple cluster rules. The clusters are formed identically for the spin up and spin down fermions. We can thus group all the clusters into pairs that are identical except for having different spin. Flipping both clusters to be in the same orientation then gives an identical fermion sign for each spin sector, thus canceling each other out. No matter how the clusters are shaped, we can always flip them to be in a “reference configuration” with both spin sectors identical, which will always have a positive contribution to the partition function.

The on-site attraction term proportional to U is implemented with an extra on-site plaquette similar to the mass term in the previously studied staggered fermion model [6]. Here, however, the extra link can either do nothing, or it can

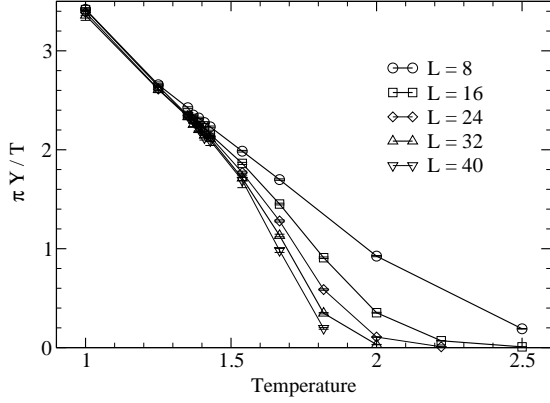


Figure 3. Winding number versus temperature for $U = 8$ and $\Delta = 1$.

freeze two clusters of different spin together in the same orientation. If frozen together the clusters can still be flipped, but both spin sectors must be flipped together. Note that this frozen state is consistent with the reference configuration which allows us to include it in the meron-cluster algorithm. This also limits us to studying an on-site attraction in this model since a repulsion would need to freeze the clusters in opposite orientations which is contrary to the reference configuration.

4. Numerical Results

We simulated the model presented above using a variant of the implementation used in [6,7]. We have been able to simulate systems with a spatial volume (V) of 128^2 , but we will only present results of up to 64^2 here. Each simulation produced between 10^5 and 10^6 configurations after performing at least 10^4 thermalization sweeps. In all cases we measured the autocorrelation time to be less than two configurations.

The transition to a state with long range order can be seen in the S-wave pair correlation

$$P_L = \frac{2}{Z\beta V} \int_0^\beta \text{Tr} \left[e^{-(\beta-t)H} p^- e^{-tH} p^+ \right] \quad (7)$$

with

$$p^+ = \sum_x c_{x,\uparrow}^\dagger c_{x,\downarrow}^\dagger, \quad p^- = (p^+)^\dagger. \quad (8)$$

In the thermodynamic limit ($L \rightarrow \infty$), the pair

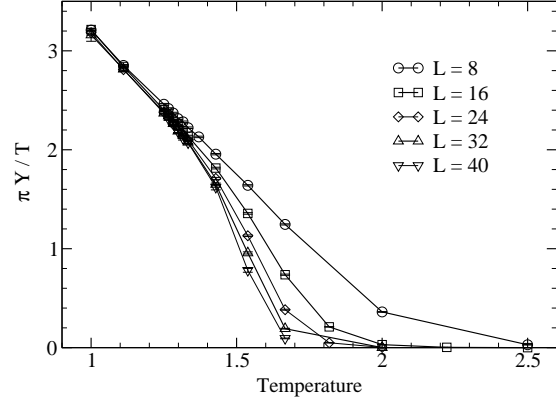


Figure 4. Winding number versus temperature for $U = 0$ and $\Delta = 1$.

correlation should diverge near a KT transition as $P_\infty \propto \xi_\infty^{7/4}$ with

$$\xi_\infty \propto \begin{cases} e^{a(T-T_c)^{-1/2}} & \text{for } T > T_c \\ \infty & \text{for } T < T_c \end{cases}. \quad (9)$$

Figures 1 and 2 show the pair correlation for $U = 8$ and $U = 0$ respectively. In both cases we can clearly see evidence of long range correlations forming. Here we do not see much of a difference between the nearly bosonic ($U = 8$) and fermionic ($U = 0$) model, only a slight shift in the critical temperature.

One could attempt to extract T_c from fitting the pair correlation for the largest volume available to the above form for P_∞ . This generally turns out to be difficult due to the large volumes necessary to approximate P_∞ near T_c .

An easier way of measuring T_c comes from the helicity modulus [8,9] which can be defined in terms of the winding number as

$$\Upsilon = \frac{T}{2} \langle W_x^2 + W_y^2 \rangle \quad (10)$$

where W_x (W_y) is the total number of particles winding around the boundary in the x (y) direction. This is very convenient to work with since we know the finite size scaling form to be

$$\frac{\pi}{T} \Upsilon = A(T) \left[2 + \frac{1}{\log(L/L_0(T))} \right] \quad (11)$$

with $A(T_c) = 1$. In figures 3 and 4 we show the quantity $\pi\Upsilon/T$ for the two different values of U .

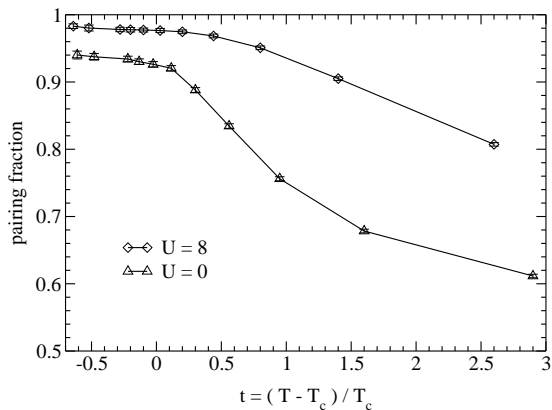


Figure 5. Pairing fraction versus reduced temperature for ($U = 8$) and fermionic ($U = 0$) limits.

Here we can clearly see the tendency of a universal jump between 0 and 2 at T_c . Near T_c we can fit the helicity modulus for several volumes to (11) to get the two parameters $A(T)$ and $L_0(T)$. We see that the coefficient $A(T)$ moves approximately linearly through 1 as T goes through T_c . By fitting a straight line to $A(T)$ we can determine T_c . For $U = 8$ we estimate that $T_c = 1.39(2)$ while for $U = 0$ we get $T_c = 1.28(2)$.

For $\Delta = 1$ with $U \rightarrow \infty$ our model maps onto the quantum XY model with an extra factor of $1/4$ multiplying the temperature. Scaling the measured result for the XY model [9], we should get $T_c = 1.3708(2)$ for large enough U . Our result for $U = 8$ is consistent with this which provides a good check of our simulations. We also see that $U = 8$ is indeed close to the bosonic limit.

We can better understand how the model changes as we adjust U by measuring the pairing fraction which we define as

$$f = 2 \langle n_\uparrow n_\downarrow \rangle / \langle n_\uparrow + n_\downarrow \rangle . \quad (12)$$

In figure 5 we show the pairing fraction for both $U = 8$ and $U = 0$ versus the reduced temperature $t = (T - T_c) / T_c$ using T_c as determined above. Here we can distinctly see the effects of the on-site attraction. For $U = 8$ the pairing fraction gradually increases as T_c is approached from above and comes within a few percent of its value at T_c well before the KT transition. For $U = 0$ we see a more dramatic rise as T_c is ap-

proached from above. Here the pairing fraction levels off much closer to T_c than for $U = 8$, but still just before the transition.

5. Conclusions

We have efficiently simulated a fermionic model with the same symmetries as the attractive Hubbard model. In this model we observed a KT transition at a finite temperature for $\Delta = 1$ in the bosonic ($U=8$) and fermionic ($U=0$) limits. By measuring the helicity modulus, we were able to easily obtain the critical temperature.

In the future we will include a chemical potential in our simulations. This will allow us to move away from half filling. We also plan to study this model in 3 dimensions to observe the physics of massless Goldstone bosons.

Acknowledgements

We would like to thank U.-J. Wiese for motivating discussions. A majority of the simulations were performed on computers generously donated by Intel Corporation.

REFERENCES

1. S. Chandrasekharan and U.-J. Wiese, Phys. Rev. Lett. 83 (1999) 3116.
2. See for example, M. Randeria, cond-mat/9710223.
3. A. Moreo and D.J. Scalapino, Phys. Rev. Lett. 66 (1991) 946; R. Lacaze, et. al., cond-mat/9610193.
4. S. Chandrasekharan and J.C. Osborn, in preparation.
5. S. Chandrasekharan, et. al., Nucl. Phys. B 576 (2000) 481; S. Chandrasekharan, Nucl. Phys. Proc. Suppl. 83 (2000) 774; J. Cox, et. al., Nucl. Phys. Proc. Suppl. 83 (2000) 777.
6. S. Chandrasekharan and J.C. Osborn, hep-lat/0010036.
7. J.C. Osborn, "Meron Cluster Updates with Binary Trees", in preparation.
8. E.L. Pollock and D.M. Ceperley, Phys. Rev. B 36 (1987) 8343; H. Weber and P. Minnhagen, Phys. Rev. B 37 (1988) 5986.
9. K. Harada and N. Kawashima, J. Phys. Soc. Jpn. 67 (1998) 2768.